Int. J. Electrochem. Sci., 4 **(2009)** 551 - 561

International Journal of ELECTROCHEMICAL SCIENCE
www.electrochemsci.org

Parameterization and Determination of the Electrode Potentials of Levodopa: Computational Study

Siavash Riahi [1,2,*], *Solmaz Eynollahi*[2], *Mohammad Reza Ganjali*[2]

[1] Institute of Petroleum Engineering, Faculty of Engineering, University of Tehran
[2] Center of Excellence in Electrochemistry, Faculty of Chemistry, University of Tehran, P. O. Box 14155-6455, Tehran, Iran
[*]E-mail: riahisv@khayam.ut.ac.ir

Received: 2 March 2008 / *Accepted:* 13 March 2009 / *Published:* 22 March 2009

Formal potential of levodopa in aqueous solution is computed theoretically using second order Møller–Plesset perturbation theory. The calculations are carried out at the MP2 level by continuum solvation method of PCM to mimic the role of solvent. The calculated values were compared with the experimental values obtained by linear sweep voltammetry. Cyclic voltammograms of levodopa show a redox couple with anodic and cathodic peak potentials at 0.58V and 0.52 V (vs. Ag/AgCl), respectively. The observed and the calculated changes in the reduction potential of the levodopa differed from those of the reference compound (catechol), being less than 14 mV. In this way, a method was provided, by which the reduction potentials of the related molecules could be predicted very accurately. Actually, the resulting data illustrated that the method was likely to be useful for the prediction of biomolecules electrode potentials in different aprotic solvents. The bond lengths, bond angles and dipole moment of levodopa were calculated in water.

Keywords: Redox reaction, Ab initio calculation, Levodopa, Chemometrics, MP2

1. INTRODUCTION

Levodopa (3,4-dihydroxy-L-phenylalanine) is a naturally occurring amino acid found in food and made from L-Tyrosine in the human body. Levodopa (LD) is converted into dopamine in the brain and body. It is sold as a dietary supplement and as a prescription drug in the US. In clinical use, Levodopa is administered in the management of Parkinson's disease and dopa-responsive dystonia. It is also used as a component in marine adhesives used by pelagic life.

Parkinson's disease (PD) is a degenerative disease of brain and up to now approximately 500,000 people in the United States have been diagnosed with it. Neurotransmitters, especially

dopamine, play a significant role in the research of PD. In the past decade, extensive work has been carried out on it [1].

Some studies suggest a cytotoxic role in the promotion and occurrence of adverse effects associated with levodopa treatment [2]. Though the drug is generally safe in humans, some researchers have reported an increase in cytotoxicity markers in rat pheochromocytoma PC12 cell lines treated with levodopa [3]. Other authors have attributed the observed toxic effects of levodopa in neural dopamine cell lines to enhanced formation of quinones through increased auto-oxidation and subsequent cell death in mesencephalic cell cultures [4, 5].

For these reasons, knowledge of the redox properties of LD is important for a better understanding of their behavior in biological environments.

The electro-oxidation of the compound in this category is well documented and involves a transfer of two electrons and two protons to provide the associated quinones [6-7].

The electron transfer process constitutes the basic feature of chemical, biochemical and, especially, electrochemical reactions. Therefore, the ability to calculate redox potentials accurately using the theoretical methods would be advantageous in a number of different areas, particularly where the experimental measurements are difficult, due to the complex chemical equilibria and the reactions of the involved chemical species. Recently, a number of reports, dealing with the electrode potential calculation of several biomolecules, have been published in the literature [8-11]. In recent years, our research group has been involved in the different branch of chemical and electrochemical sciences [12-28].

Solvent effects often play an important role in the molecule's geometry. The self-consistent reaction field (SCRF) theory [29] has been quite successful in describing the solvent effects on the molecules in solution. This theory has been applied in this work along with MP2 method for the molecular parameterization and calculation of electrode potentials of the studied compounds [30].

In this paper, the standard electrode potentials for levodopa in water was calculated with the employment of ab initio molecular orbital calculations with 6-31G* basis set. Additionally, comparison of the resulting data with the experimental values is presented. Since the solvation energy of the organic molecules plays a critical role in their reactivity, the solvation energy calculations of the studied molecules in water are also of interest. Furthermore, solvent effects on geometry and also dipole moment were studied.

2. CALCULATION AND EXPERIMENTAL DETAILS

2.1. Calculations

Scheme 1 depicts the two-electron oxidation reaction of the levodopa, ($LD(OH)_2$).

The oxidized form ($LD(O)_2$) can also be converted to its reduced form ($LD(OH)_2$) using catechol $CA(OH)_2$ as a reference molecule, according to the following isodesmic reaction [31]:

$$LD(O)_{2\,(sol)} + CA(OH)_{2\,(sol)} \longrightarrow LD(OH)_{2\,(sol)} + CA(O)_{2\,(sol)} \qquad (1)$$

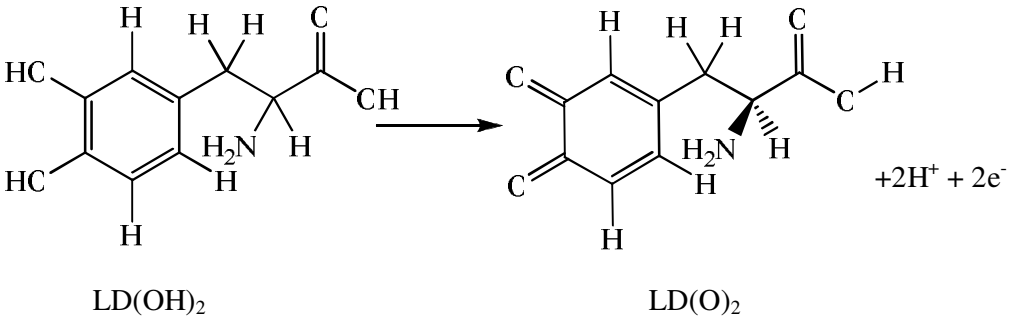

Scheme 1. Electron oxidation reaction which is for LD

The difference between the electrode potential of the two species can be obtained from the change in the Gibbs free energy of reaction (1), in accordance with the equation (2):

$$E^{o\prime} = E^{o'}_{CA} - \frac{\Delta G^{\circ}}{2F} \qquad (2)$$

Where ΔG° is the free energy change for reaction (1), $E^{o\prime}_{CA}$ is the experimental formal electrode potential for a reference molecule, $E^{o\prime}$ is the calculated electrode potential and F is the Faraday constant. The Gibbs free energy change for reaction (1) can be computed by the thermodynamic cycle depicted in Figure 1, which is used in the case of transferring all the involved species in the reaction from the gas phase into the solution phase [32].

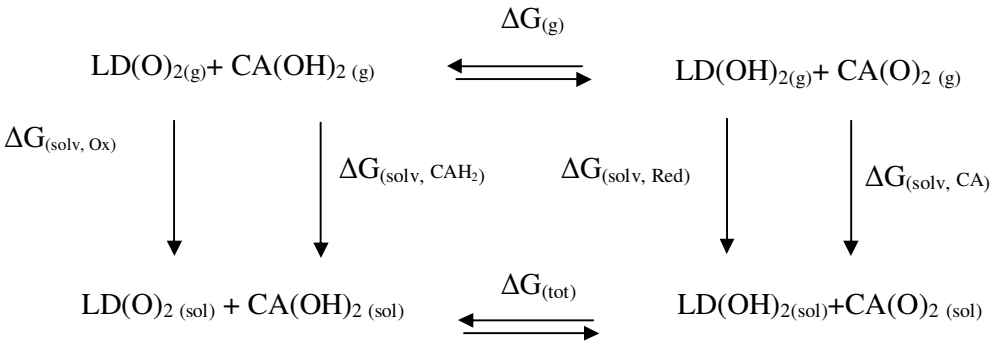

Figure 1. The thermodynamic cycle, proposed to convert the standard Gibbs energy of the isodesmic redox reaction in the gas phase to the standard Gibbs energy of the reaction in solution.

In order to calculate the standard Gibbs energy of reaction (1), ΔG°, one should calculate the standard Gibbs energy of each component, ΔG_i°, in reaction (1):

$$\Delta G^{\circ} = \sum \nu_i \Delta G_i^{\circ} \quad (3)$$

where ΔG_i° the standard Gibbs energy of each component and ν_i is the stoichiometric coefficient. The standard Gibbs energy of each component is obtained using the following expression:

$$\Delta G_i^o = \Delta G_{i,gas}^o + \Delta G_{i,solv}^o \quad (4)$$

where $\Delta G_{i,gas}^o$ is the gas-phase energy of each component and $\Delta G_{i,solv}^o$ is the solvation energy of the component. In the present work, the gas-phase contribution to the Gibbs energy, $\Delta G_{i,gas}^o$, was determined from ab initio calculation. This calculation have been performed at the Møller–Plesset perturbation theory using the 6-31G * basis set [33-35]. The zero-point energies and thermal corrections together with entropies have been used to convert the internal energies to the Gibbs energies at 298.15 K. Solvation energies, $\Delta G_{i,solv}^o$, have been calculated using Polarisable Continuum Model (PCM) [36].

2.2. Softwares and equipments

The formal potentials (E°´) were calculated as the average of the anodic and cathodic peak potentials of the cyclic voltammogram ($(E_{pa} + E_{pc})/2$) at 25 $mV.s^{-1}$[37]. All experiments were carried out at 25±1 ºC temperature.

A Pentium IV personal computer (CPU at 3.06 GHz) with the Windows XP operating system was used. The initial geometry optimization was performed with HyperChem (Version 7.0 Hypercube, Inc., Alberta, Canada). For all the ab initio calculation, Gaussian 98 has been employed [38].

3. RESULTS AND DISCUSSION

The geometrical optimization was the most significant step for the calculation of the formal electrode potential, on the grounds that the molecular parameters were controlled by the molecular geometry.

The bond lengths and bond angles of the studied compounds were optimized in water (Figures 2a and 2b). Tables 1 shows the structural characteristics of $LD(O)_2$ and $LD(OH)_2$ in the gas and solution phase.

C-O and O-H bond lengths in solvent are more than those in gas for $LD(O)_2$ and $LD(OH)_2$. Water is a protic solvent which makes strong hydrogen bonding with -OH groups in the structure of the studied molecules. Formation of hydrogen bonding cause displacement in the electronic density from C-O and O-H bonds toward water molecule and makes these bonds weak and therefore increases the bond lengths. For example in $LD(O)_2$, R(12,14) from 1.3885 to 1.3984, R(12,13) from 1.217 to

1.2385 and , R(14,23) from 0.9901 to 1.1014 and in $LD(OH)_2$, R(12,13) from 1.217 to 1.2286, R(12,14) from 1.3902 to 1.403 and , R(14,24) from 0.9903 to 1.1024 are changed.

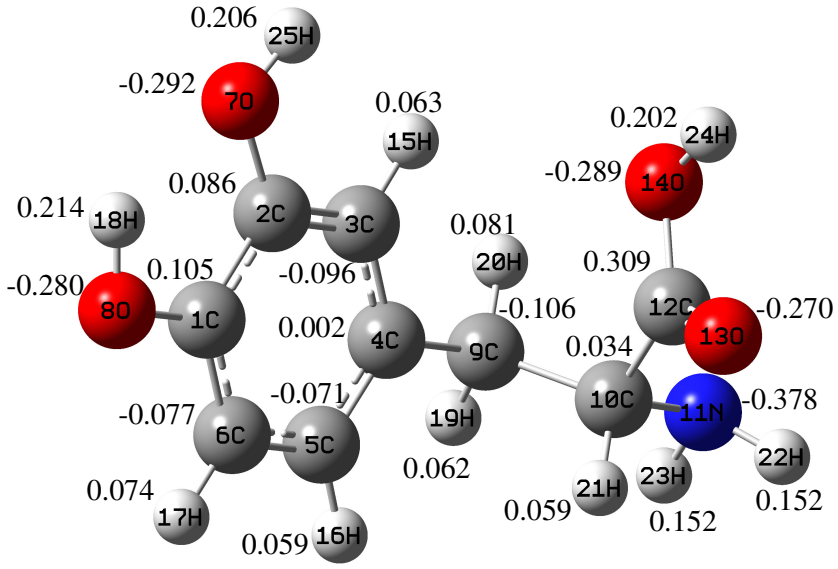

(*a*)

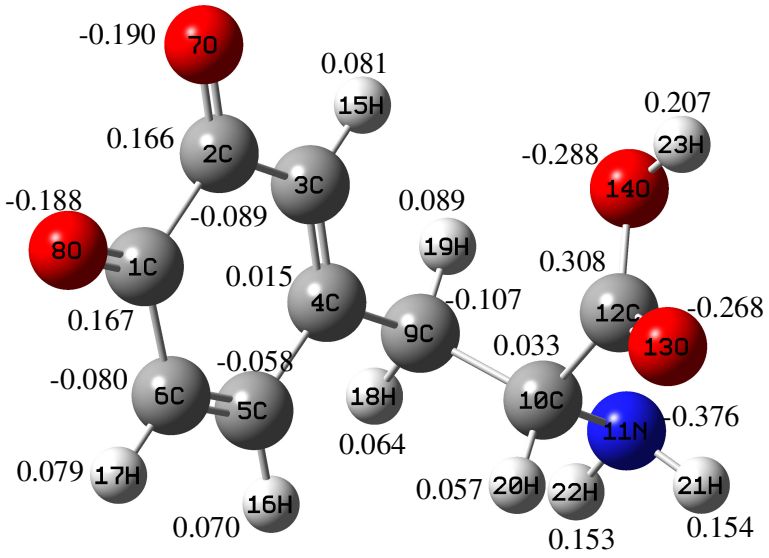

(*b*)

Figure 2. Optimized structures and atomic charges of (*a*) LD(ox) and (*b*) LD(red) in water.

Comparing the bond angles in both $LD(O)_2$ and $LD(OH)_2$, it can be concluded that angles on which hydrogen bonding affect, for example in $LD(O)_2$ A(12,14,23) from 104.5346 to 105.98, A(10,11,22) from 107.4317 to 106.298 and in $LD(OH)_2$ A(2,7,25) from 105.793 to 106.779, A(22,11,23) from 104.611 to 103.639 are changed. C-O bond length decreased from $LD(OH)_2$ to $LD(O)_2$ (from 1.2376Å to 1.4203Å) in both C-O bonds in ring. The reason is that the C-O bonding in Red form change into C=O bonding in Ox form.

Table 1. The structural characteristics of $LD(O)_2$ and $LD(OH)_2$ in gas and solvent

	$LD(O)_2$			$LD(OH)_2$	
	Gas	Solvent		Gas	Solvent
Bond length (Å)			Bond length (Å)		
R(1,2)	1.5481	1.5501	R(1,2)	1.4048	1.4059
R(1,6)	1.5055	1.5035	R(1,6)	1.3865	1.3864
R(1,8)	1.2267	1.2371	R(1,8)	1.3945	1.4105
R(2,3)	1.5044	1.5022	R(2,3)	1.3839	1.3853
R(2,7)	1.2272	1.2366	R(2,7)	1.4001	1.4203
R(3,4)	1.3250	1.3256	R(3,4)	1.3930	1.3931
R(3,15)	1.0830	1.0840	R(3,15)	1.0826	1.0838
R(4,5)	1.4902	1.4910	R(4,5)	1.3883	1.3881
R(4,9)	1.5300	1.5299	R(4,9)	1.5301	1.5302
R(5,6)	1.3207	1.3211	R(5,6)	1.3874	1.3874
R(5,16)	1.0839	1.0857	R(5,16)	1.0822	1.0831
R(6,17)	1.0833	1.0845	R(6,17)	1.0819	1.0831
R(9,10)	1.5535	1.5550	R(7,25)	0.9869	1.0201
R(9,18)	1.0895	1.0898	R(8,18)	0.9897	1.0321
R(9,19)	1.0866	1.0870	R(9,10)	1.5539	1.5557
R(10,11)	1.4925	1.4932	R(9,19)	1.0888	1.0890
R(10,12)	1.5541	1.5549	R(9,20)	1.0869	1.0874
R(10,20)	1.0962	1.0965	R(10,11)	1.4933	1.4933
R(11,21)	1.0337	1.0363	R(10,12)	1.5535	1.5542
R(11,22)	1.0333	1.0360	R(10,21)	1.0962	1.0966
R(12,13)	1.2170	1.2385	R(11,22)	1.0338	1.0363
R(12,14)	1.3885	1.4020	R(11,23)	1.0333	1.0359
R(14,23)	0.9901	1.1014	R(12,13)	1.2170	1.2286
			R(12,14)	1.3902	1.4030
Bond angles(°)			R(14,24)	0.9903	1.1020
A(2,1,6)	116.0029	116.123	Bond angles(°)		
A(2,1,8)	121.0702	120.562			
A(6,1,8)	122.9268	123.315	A(2,1,6)	119.121	119.253
A(1,2,3)	116.4995	116.593	A(2,1,8)	120.848	121.238
A(1,2,7)	120.7483	120.322	A(6,1,8)	120.032	119.509
A(3,2,7)	122.7522	123.086	A(1,2,3)	120.258	119.938
A(2,3,4)	122.4795	122.253	A(1,2,7)	115.082	115.405
A(2,3,15)	116.1136	116.145	A(3,2,7)	124.661	124.657
A(4,3,15)	121.4068	121.603	A(2,3,4)	120.569	120.738
A(3,4,5)	120.5251	120.684	A(2,3,15)	119.487	118.958

Table 1. (continued)

	Gas			DPID	
	B3LYP	HF		B3LYP	HF
Bond angles(°)			Bond angles(°)		
A(3,4,9)	122.0498	122.054	A(4,3,15)	119.944	120.304
A(5,4,9)	117.4248	117.262	A(3,4,5)	118.834	118.904
A(4,5,6)	122.8303	122.866	A(3,4,9)	120.440	120.506
A(4,5,16)	116.8621	116.757	A(5,4,9)	120.724	120.584
A(6,5,16)	120.3061	120.376	A(4,5,6)	121.100	120.929
A(1,6,5)	121.6620	121.481	A(4,5,16)	119.675	119.701
A(1,6,17)	116.5006	116.630	A(6,5,16)	119.224	119.370
A(5,6,17)	121.8373	121.888	A(1,6,5)	120.119	120.239
A(4,9,10)	112.6562	112.625	A(1,6,17)	119.048	119.096
A(4,9,18)	109.3416	109.253	A(5,6,17)	120.833	120.665
A(4,9,19)	110.0537	109.851	A(2,7,25)	105.793	106.779
A(10,9,18)	108.1615	108.087	A(1,8,18)	103.939	104.762
A(10,9,19)	108.4415	108.766	A(4,9,10)	112.869	112.688
A(18,9,19)	108.0644	108.146	A(4,9,19)	109.535	109.659
A(9,10,11)	109.1835	109.154	A(4,9,20)	110.365	110.195
A(9,10,12)	111.5456	110.849	A(10,9,19)	107.724	107.727
A(9,10,20)	109.5800	109.323	A(10,9,20)	108.351	108.532
A(11,10,12)	107.9047	108.620	A(19,9,20)	107.837	107.897
A(11,10,20)	112.1018	112.213	A(9,10,11)	109.376	109.448
A(12,10,20)	106.5183	106.672	A(9,10,12)	112.014	110.985
A(10,11,21)	107.4317	106.765	A(9,10,21)	109.273	109.006
A(10,11,22)	107.1460	106.298	A(11,10,12)	107.644	108.618
A(21,11,22)	104.6840	104.095	A(11,10,21)	112.084	112.209
A(10,12,13)	125.3389	125.282	A(12,10,21)	106.448	106.559
A(10,12,14)	112.5449	112.308	A(10,11,22)	107.405	106.823
A(13,12,14)	122.1100	122.409	A(10,11,23)	107.046	106.311
A(12,14,23)	104.5346	105.98	A(22,11,23)	104.611	103.639
A(3,4,9)	122.0498	122.054	A(10,12,13)	125.487	125.373
A(5,4,9)	117.4248	117.262	A(10,12,14)	112.793	112.393
			A(13,12,14)	121.709	122.234
			A(12,14,24)	104.325	105.929

For both the reduced and oxidized forms in the gas and solution phases, the calculated Gibbs energies of the molecules are summarized in Table 2, using frequency calculation MP2 theory level. For the selection of 6-31G* basis set, the decisive factor was the size of the studied molecules. The computation of the solvation energies is considered an essential step, since these energy values are required for the conversion of the gas-phase energies to the energies in the solution phase. As a matter of fact, these solute–solvent interactions, calculated by the PCM solvation model [36], were added to the gas phase energies to give the Gibbs energy change of each component in the solution phase. Table 2 also lists the total Gibbs free energy of each component in the presence of water.

Table 2. The Gibbs free energy of the studied molecules for both reduced (red.) and oxidized (ox.) forms in the gas phase and the solution phase, along with the change of the Gibbs free energy of reaction (1), ΔG_i^{o}, in both gas and solution phases [a]

	Mol.	$\Delta G^{o}_{i,gas}$ [b]		$\Delta G^{o}_{i,solv}$ [b]		ΔG_i^{o} (kJ/mol)	
		Red.	Ox.	Red.	Ox.	Gas	Solution
MP2/	LD	-691.94277	-690.74601	-691.96865	-690.76799	-44.5258503	77.8408166
6-31G(d)*	CA	-380.95453	-379.77474	-380.98108	-379.78978	0	0

[a] Solution result was obtained with the PCM model

[b] These energies are in atomic units, Hartree (1 Hartree = 2625.49975 kJ mol^{-1})

The attainment of LD electrode potentials was achieved with the aid of the total Gibbs energies and the experimental value of the electrode potential of the reference molecule, catechol (CA), in water (Eq. (2)) [8-11]. Table 3 presents the electrode potentials of the molecules, studied in water at the MP2/6-31G* level. According to this Table, the electrode potentials of the molecules at this method and those obtained through experiments were found to be in a satisfactory agreement.

Table 3. Electrode potentials of the studied molecules, compared with the experimental values[a]. The differences (in mV) between the experimental and the calculated values are presented.

Mol.[b]	Exp.(E°´(mV)) [c]	E°´ (mV)[d] (MP2/6-31G(d)*)
LD	189	203
CAH_2	375	375

[a] Calculated by Equation 2 ($E^{o\prime} = E^{o'}_{CA} - \frac{\Delta G^{\circ}}{2F}$)

[b] Studied Molecules

[c] Experimental values.

[d] Electrode potentials calculated by Eq. (2) as explained in the text

Table 4 summarizes the highest occupied molecular orbital (HOMO), the lowest unoccupied molecular orbital (LUMO) and HOMO and LUMO energy gaps for LD calculated at MP2 level in the 6-31G(d)* basis set. The eigenvalues of LUMO and HOMO and their energy gap reflect the chemical activity of the molecule. LUMO as an electron acceptor represents the ability to obtain an electron, while HOMO as an electron donor represents the ability to donate an electron. The smaller the LUMO and HOMO energy gaps, the easier it is for the HOMO electrons to be excited; the higher the HOMO energies, the easier it is for HOMO to donate electrons; the lower the LUMO energies, the easier it is for LUMO to accept electrons. From the resulting data shown in table 4, it is obvious that the LUMO energies of LD are lower than those of CA and the energy gap of LD is smaller than that of CA. Consequently, the electrons transfer from HOMO to LUMO in LD is relatively easier than that in CA. With the decrease of the LUMO energies, LUMO in LD accepts electrons easily. The same methods

were employed to study LD, also leading to the above stated conclusions and confirming the obtained results. Furthermore, dipole moment was calculated in the solvent and is shown in Table 4.

Table 4. The calculated amounts of HOMO and LUMO energies with the MP2/6-31G(d)* basis set and Dipole moment of the studied molecules in solvents with the 6-31G(d)* basis set (μ,Debye)

	E_{HOMO} (eV)	E_{LUMO}(eV)	E_{LUMO}-E_{HOMO} (eV)	Dipole Moment
$LD(OH)_2$	-6.20846	6.319215	12.52768	2.0313
$LD(O)_2$	-7.45037	4.03648	11.48685	4.9631
$CA(OH)_2$	-6.35894	7.194316	13.55326	1.4905
$CA(O)_2$	-7.62561	3.959473	11.58508	4.0045

4. CONCLUSIONS

For LD the formal electrode potentials was predicted with the help of MP2 level with the 6-31G(d)* basis set. It was revealed that the data from the experiments coincided with the predicted formal electrode potentials for the LD half reactions. The average discrepancy between the theoretical and the experimental values was less than 14 mV. This theoretical method is very effective for the prediction of an unknown formal electrode potential of any compound involved in biochemistry.

Unfortunately, it is a fact that the molecular geometrical optimization in the presence of a solvent, using the PCM solvation model at the same theory level, required a substantial amount of time for computations. Subsequently, further theory refinement should be conducted, principally on this matter. Since water make strong hydrogen bonding, it affects bonds contain oxygen atom.

References

1. Z. G. Liu, W. S. Sun, Z. F. Weng, M. H. Shen, P. Y. Li, Q. F. Kuang, H. L. Fu, C. M. Zhu and S. D. Chen, *Natl. Med. J. Chin.*, 80 (2000) 392.
2. N. -N. Cheng, T. Maeda, T. Kume, S. Kaneko, H. Kochiyama, A. Akaike, Y. Goshima and Y. Misu, *Brain res.,* 743 (1996) 278.
3. A. N. Basma, E. J. Morris, W. J. Nicklas and H. M. Geller, *J. Neurochem.*, 64 (1995) 825.
4. B. Pardo, M. A. Mena, M. J. Casarejos, C. L. Paino and J. G. De Yebenes, *Brain res.*, 682 (1995) 133.
5. C. Mytilineou, S. K. Han and G. Cohen, *J. Neurochem.*, 61 (1993) 1470.
6. H. H. W. Thijssen, *Pestic. Sci.*, 43 (1995) 73.
7. S. Riahi, M. R. Ganjali, A. B. Moghaddam, P. Norouzi, G. R. Karimipour and H. Sharghi, *Chem. Phys.*, 337 (2007) 33.
8. S. Riahi, M. R. Ganjali, A. B. Moghaddam and P. Norouzi, *J. Theor. Comput. Chem. (JTCC)*, 6 (2007) 331.
9. S. Riahi, M. R. Ganjali, A. B. Moghaddam and P. Norouzi, *J. Theor. Comput. Chem. (JTCC)*, 6 (2007) 255.

10. S. Riahi, M. R. Ganjali, A. B. Moghaddam and P. Norouzi, *Spectrochim. Acta, Part A*, 71 (2008) 1390.
11. S. Riahi, A. B. Moghaddam, M. R. Ganjali and P. Norouzi, *Int. J. Electrochem. Sci*., 4 (2009) 122.
12. M. R. Ganjali, P. Norouzi, F. S. Mirnaghi, S. Riahi and F. Faridbod, *IEEE Sens. J*., 7 (2007) 1138.
13. S. Riahi, M. R. Ganjali, A. B. Moghaddam and P. Norouzi, *Spectrochim. Acta, Part A*, 70 (2008) 94.
14. S. Riahi, M. R. Ganjali, P. Norouzi and F. Jafari, *Sens. Actuators, B*, 132 (2008) 13.
15. F. Faridbod, M. R. Ganjali, B. Larijani, P. Norouzi, S. Riahi and F. Sadat Mirnaghi, *Sensors*, 7 (2007) 3119.
16. S. Riahi, M. R. Ganjali and P. Norouzi, *J. Theor. Comput. Chem. (JTCC)*, 7 (2008) 317.
17. F. Faridbod, M. R. Ganjali, R. Dinarvand, P. Norouzi and S. Riahi, *Sensors*, 8 (2008) 1645.
18. S. Riahi, A. B. Moghaddam, P. Norouzi and M. R. Ganjali, *J. Mol. Struct. (THEOCHEM)*, 814 (2007) 131.
19. S. Riahi, M. R. Ganjali, A. B. Moghaddam and P. Norouzi, *J. Mol. Struct. (THEOCHEM)*, 896 (2009) 63.
20. M. F. Mousavi, M. Shamsipur, S. Riahi and M. S. Rahmanifar, *Anal. Sci*., 18 (2002) 137.
21. S. Riahi, M. F. Mousavi, M. Shamsipur and H. Sharghi, *Electroanal*., 15 (2003) 1561.
22. A. Moosavi-Movahedi, S. Safarian, G. H. Hakimelahi, G. Ataei, D. Ajloo, S. Panjehpour, S. Riahi, M. F. Mousavi, S. Mardanyan, N. Soltani, A. Khalafi-Nezhad, H. Sharghi, H. Moghadamnia and A. A. Saboury, *Nucleos. Nucleot. Nucl*., 23 (2004) 613.
23. H. Karami, M. F. Mousavi, M. Shamsipur and S. Riahi, *J. Power Sources*, 154 (2006) 298.
24. M. R. Ganjali, P. Norouzi, F. Faridbod, S. Riahi, J. Ravanshad, J. Tashkhourian, M. Salavati-Niasari and M. Javaheri, IEEE Sens. J., 7 (2007) 544.
25. M. R. Ganjali, T. Razavi, R. Dinarvand, S. Riahi and P. Norouzi, *Int. J. Electrochem. Sci*., 3 (2008) 1543.
26. M. R. Ganjali, M. Tavakoli, F. Faridbod, S. Riahi, P. Norouzi and M. Salavati-Niassari, *Int. J. Electrochem. Sci*., 3 (2008) 1559.
27. M. R. Ganjali, M. Hariri, S. Riahi, P. Norouzi and M. Javaheri, *Int. J. Electrochem. Sci*., 4 (2009) 295.
28. S. Riahi, F. Faridbod and M. R. Ganjali, *Sensor Lett*. 7 (2009) 42.
29. S. Riahi, A. Bayandori Moghaddam, M. R. Ganjali and P. Norouzi, *J. Theor. Comput. Chem. (JTCC)*, 6 (2007) 331.
30. O. Tapia and O. Goscinski, *Mol. Phys*., 29 (1975) 1653.
31. M. W. Wong, K. B. Wiberg and M. J. Frisch, *J. Am. Chem. Soc*., 114 (1992) 1645
32. M. Namazian and P. Norouzi, *J. Electroanal. Chem*., 573 (2004) 49.
33. R. J. Driebergen, J. J. M. Holthuis, J. S. Blauw, S. J. Postma. Kelder., W. Verboom, D. N. Reinhoud and W. E. Van der Linden, *Anal. Chim. Acta*, 234 (1990) 285.
34. J. B. Foresman and A. E. Frisch, Gaussian Inc, Pittsburgh, PA (1998).
35. D. C. Young, Computational Chemistry, A Practical Guide for Applying Techniques to Real-World Problems, John Wiley & Sons, Inc., New York (2000).
36. C. J. Cramer, Essentials of Computational Chemistry: Theories and Models, 2nd ed, Wiley, Chichester (2004).
37. M. S. M. Quintino, M. Yamashita and L. Angnes, *Electroanal*., 18 (2006) 655.
38. M. J. Frisch, G. W. Trucks, H. B. Schlegel, G. E. Scuseria, M. A. Robb, J. R. Cheeseman, V. G. Zakrzewski, J. A. Montgomery, R. E. Stratmann, J. C. Burant, S. Dapprich, J. M. Millam, A. D. Daniels, K. N. Kudin, M. C. Strain, O. Farkas, J. Tomasi, V. Barone, M. Cossi, R. Cammi, B. Mennucci, C. Pomelli, C. Adamo, S. Clifford, J. Ochterski, G. A. Petersson, P. Y. Ayala, Q. Cui, K. Morokuma, D. K. Malick, A. D. Rabuck, K. Raghavachari, J. B. Foresman, J. Cioslowski, J. V. Ortiz, B. B. Stefanov, G. Liu, A. Liashenko, P. Piskorz, I. Komaromi, R. Gomperts, R. L. Martin, D. J. Fox, T. Keith, M. A. Al-Laham, C. Y. Peng, A. Nanayakkara, C. Gonzalez, M. Challacombe,

P. M. W. Gill, B. Johnson, W. Chen, M. W. Wong, J. L. Andres, C. Gonzalez, M. Head-Gordon, E. S. Replogle, and J. A. Pople, Gaussian, Inc., Pittsburgh PA (1998).